International Journal of Power Electronics and Drive System (IJPEDS)
Vol. 6, No. 3, September 2015, pp. 648~656
ISSN: 2088-8694

Modeling and Simulation of Closed Loop Controlled Parallel Cascaded Buck Boost Converter Inverter Based Solar System

T. Sundar*, S. Sankar**
* Dept. of EIE, SCSVMV University, Kanchipuram, Tamilnadu, India
** Dept. of EEE, Panimalar Institute of Technology, Chennai, Tamilnadu, India
Email: sundar_151@yahoo.co.in, ssankarphd@yahoo.com

Article Info

Article history:

Received Apr 27, 2015
Revised Jul 25, 2015
Accepted Aug 15, 2015

Keyword:

Bidirectional inverter
Buck/Boost Converter
DC-distribution applications
Maximum power point trackers
Sim Power System

ABSTRACT

This Work deals with design, modeling and simulation of parallel cascaded buck boost converter inverter based closed loop controlled solar system. Two buck boost converters are cascaded in parallel to reduce the ripple in DC output. The DC from the solar cell is stepped up using boost converter. The output of the boost converter is converted to 50Hz AC using single phase full bridge inverter. The simulation results of open loop and closed loop systems are compared. This paper has presented a simulink model for closed loop controlled solar system. Parallel cascaded buck boost converter is proposed for solar system.

Corresponding Author:

T. Sundar,
Research Scholar
Departement of Electronic and Instrumentation Engineering,
SCSVMV University,
Enathur, Kanchipuram, Tamilnadu, India.
Email: sundar_151@yahoo.co.in

1. INTRODUCTION

A DC-DC converter is a vital part of alternative and renewable energy conversion, portable devices, and many industrial processes. It is essentially used to achieve a regulated DC voltage from an unregulated DC source which may be the output of a rectifier or a battery or a solar cell etc. Nevertheless, the variation in the source is significant, mainly because of the variation in the line voltage, running out of a battery etc., but within a specified limit. Taking all these into account, the objective is to regulate the voltage at a desired value while delivering to a widely varying load. A DC-DC switching regulator is known to be superior over a linear regulator mainly because of its better efficiency and higher current-driving capability. There are various topologies in the context of DC-DC converters the buck-boost converter are widely used. The basic circuit of buck-boost converter is shown in Figure 1. The output voltage of a DC-DC converter is controlled by operating it in the closed loop, and altering its MOSFET (switch) gate signal accordingly. It is basically governed by a switching logic, thus constituting a set of subsystems depending upon the status (on-off) of the switch. In the well known pulse width modulation (PWM) technique, the control is accomplished by varying the duty ratio of an external fixed frequency clock through one or more feedback loops, whenever any parameter varies. PI controllers are the most widely-used type of controller for industrial applications. They are structurally simple and exhibit robust performance over a wide range of operating conditions. In the absence of the complete knowledge of the process, these types of controllers are the most efficient choices. Power- Management strategies for a grid connected PV-FC hybrid system [1]. Optimized wind energy harvesting system using resistance emulator and active rectifier for wireless sensor nodes [2]. A hybrid cascade converter topology with series-connected symmetrical and asymmetrical diode-clamped H-Bridge cells [3]. An efficient high-step-up interleaved DC-DC converter with a common active clamp [4]. Transformerless grid connected power converter for PV system [5, 6]. Adaptive fuzzy controlled wind energy system [8]. Distribution voltage control for DC microgrid using stored energy [9]. Predictive controlled bi-directional inverter for microgrid applications [10]. Characterization and testing of a tool for photovoltaic panel modeling [11]. Analysis and simulation of characteristics and maximum power point tracking for photovoltaic systems [12]. Comparison of photovoltaic array maximum power point tracking techniques [13]. New Approach to Photovoltaic Arrays Maximum Power Point Tracking [14]. Modeling and Control for a Bidirectional Buck– Boost Cascade Inverter [15]. A Multilevel Inverter for Photovoltaic Systems with Fuzzy Logic Control [16]. A Direct DC-link Boost Voltage PID-like FuzzyControl Strategy in Z-Source Inverter [17]. A Maximum Power Point Tracking of PV System by Scaling Fuzzy Control [18]. A closed -Loop Maximum power point Tracker for Sub watt Photovoltaic Panels [19]. Grid - Connected Boost-Half-Bridge Photovoltaic Micro inverter System Using Repetitive Current Control and Maximum power point tracking [20]. Stability of a boost converter fed from a photovoltaic source [21]. Unified Approach to Reliability Assessment of Multiphase DC-DC Converters in Photovoltaic Energy Conversion Systems [22]. Safety enhanced high stepup DC-DC Converter for AC Photovoltaic Module Application [23]. Optimization and design of a cascaded DC/DC Converter Devoted to gridconnected photovoltaic System [24]. Controller design for integrated PV-converter modules under partial shading conditions [25].

The above literature does not cover modelling and simulation of closed loop controlled buck boost converter inverter based system. Closed loop parallel cascaded buck boost converter inverter system is not reported in the literature. This work aims to develop closed loop simulink model for buck boost converter - inverter based solar system.

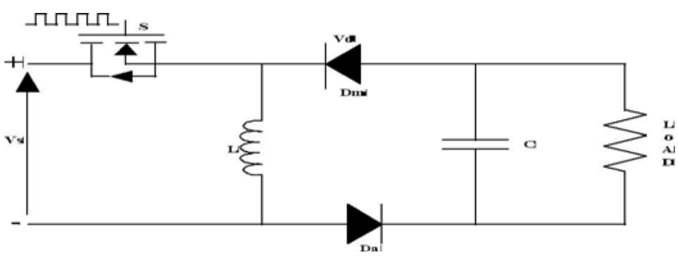

Figure 1. Schematic diagram of non-isolated buck-boost converter

2. OPERATIONAL CIRCUIT FOR BUCK-BOOST CONVERTER

The basic principle of the buck–boost converter is fairly simple while in the On-state, the input voltage source is directly connected to the inductor (L). This results in accumulating energy in L. In this stage, the capacitor supplies energy to the output load. While in the Off-state, the inductor is connected to the output load and capacitor, so energy is transferred from L to C and R. Compared to the buck and boost converters, the characteristics of the buck–boost converter are mainly polarity of the output voltage is opposite to that of the input; the output voltage can vary continuously from 0 to (for an ideal converter). The output voltage ranges for a buck and a boost converter are respectively 0 to V_i and V_i to ∞.

The buck and boost converters, the operation of the buck-boost is best understood in terms of the inductor's "reluctance" to allow rapid change in current. From the initial state in which nothing is charged and the switch is open, the current through the inductor is zero. When the switch is first closed, the blocking diode prevents current from flowing into the right hand side of the circuit, so it must all flow through the inductor. However, since the inductor doesn't like rapid current change, it initially keeps the current low by dropping most of the voltage provided by the source. Over time, the inductor allows the current to slowly increase by decreasing its voltage drop. Also during this time, the inductor stores energy in the form of a magnetic field.

2.1. CONTINUOUS MODE

If the current through the inductor *L* never falls to zero during a commutation cycle, the converter is said to operate in continuous mode.

From t=0 to t=DT, the converter is in On-State, so the switch *S* is closed. The rate of change in the inductor current (I_L) is therefore given by

$$\frac{dI_L}{dt} = \frac{V_i}{L} \quad \dots\dots\dots\dots (1)$$

At the end of the On-state, the increase of I_L is therefore

$$\Delta I_{L_{on}} = \int_0^{DT} dI_L = \int_0^{DT} \frac{V_i}{L} dt = \frac{V_i\, DT}{L} \quad \dots\dots\dots\dots (2)$$

D is the duty cycle. It represents the fraction of the commutation period *T* during which the switch is ON. Therefore *D* ranges between 0 (*S* is never on) and 1 (*S* is always on).

During the Off-state, the switch *S* is open, so the inductor current flows through the load. If we assume zero voltage drop in the diode, and a capacitor large enough for its voltage to remain constant, the evolution of I_L is

$$\frac{dI_L}{dt} = \frac{V_0}{L} \quad \dots\dots\dots\dots (3)$$

Therefore, the variation of I_L during the Off-period is

$$\Delta I_{L_{off}} = \int_0^{(1-D)T} dI_L = \int_0^{(1-D)T} \frac{V_0}{L} dt = \frac{V_0\,(1-D)T}{L} \quad \dots\dots\dots\dots (4)$$

As we consider that the converter operates in steady-state conditions, the amount of energy stored in each of its components has to be the same at the beginning and at the end of a commutation cycle. As the energy in an inductor is given by

$$E = \frac{1}{2} L I_L^2 \quad \dots\dots\dots\dots (5)$$

It is clear that the value of I_L at the end of the off state must be the same with the value of I_L at the beginning of the On-state, i.e. the sum of the variations of I_L during the on and the off states must be zero

$$\Delta I_{L_{on}} + \Delta I_{L_{off}} = 0 \quad \dots\dots\dots\dots (6)$$

Substituting $\Delta I_{L_{on}}$ and $\Delta I_{L_{off}}$ by their expressions yields

$$\Delta I_{L_{on}} + \Delta I_{L_{off}} = \frac{V_i\, DT}{L} + \frac{V_0\,(1-D)T}{L} = 0 \quad \dots\dots\dots\dots (7)$$

This can be written as

$$\frac{V_0}{V_i} = \frac{D}{D-1} \quad \dots\dots\dots\dots (8)$$

This in return yields that

$$D = \frac{V_0}{V_0 - V_i} \quad \dots\dots\dots\dots (9)$$

From the above expression it can be observed that the polarity of the output voltage is always negative (because the duty cycle goes from 0 to 1), and that its absolute value increases with D, theoretically up to minus infinity when *D* approaches 1. Apart from the polarity, this converter is either step-up (a boost converter) or step-down (a buck converter). Thus it is named a buck–boost converter.

2.2. DISCONTINUOUS MODE

In some cases, the amount of energy required by the load is small enough to be transferred in a time smaller than the whole commutation period. In this case, the current through the inductor falls to zero during part of the period. The only difference in the principle described above is that the inductor is completely discharged at the end of the commutation cycle although slight; the difference has a strong effect on the output voltage equation. It can be calculated as follows, because the inductor current at the beginning of the cycle is zero, its maximum value $I_{L_{max}}$ at (t=DT) is

$$I_{L_{max}} = \frac{V_i DT}{L} \quad \dots\dots\dots\dots (10)$$

During the off-period, I_L falls to zero after δ.T

$$I_{L_{max}} + \frac{V_0 \delta T}{L} = 0 \quad \dots\dots\dots\dots (11)$$

Using the two previous equations, δ is

$$\delta = -\frac{V_i D}{V_0} \quad \dots\dots\dots\dots (12)$$

The load current I_0 is equal to the average diode current (I_D) .The diode current is equal to the inductor current during the off-state. Therefore, the output current can be written as

$$I_0 = I_D = \frac{I_{L_{max}}}{2}\delta \quad \dots\dots\dots\dots (13)$$

Replacing $I_{L_{max}}$and δ by their respective expressions yields

$$I_0 = -\frac{V_i^2 D^2 T}{2LV_0} \quad \dots\dots\dots\dots (14)$$

Therefore, the output voltage gain can be written as

$$\frac{V_0}{V_i} = -\frac{V_i D^2 T}{2LI_0} \quad \dots\dots\dots\dots (15)$$

Compared to the expression of the output voltage gain for the continuous mode, this expression is much more complicated. Furthermore, in discontinuous operation, the output voltage not only depends on the duty cycle, but also on the inductor value, the input voltage and the output current.

The converter operates in discontinuous mode when low current is drawn by the load, and in continuous mode at higher load current levels. The limit between discontinuous and continuous modes is reached when the inductor current falls to zero exactly at the end of the commutation cycle.

In this case, the output current I_{0lim} (output current at the limit between continuous and discontinuous modes) is given by:

$$I_{0lim} = I_D = \frac{I_{L_{max}}}{2}(1 - D) \quad \dots\dots\dots\dots (16)$$

Replacing $I_{L_{max}}$ by the expression given in the discontinuous mode section yields

$$I_{0lim} = \frac{V_i DT}{2L}\,(1 - D) \quad \dots\dots\dots\dots (17)$$

As I_{0lim} is the current at the limit between continuous and discontinuous modes of operations, it satisfies the expressions of both modes. Therefore, using the expression of the output voltage in continuous mode, the previous expression can be written as:

$$I_{0lim} = \frac{V_i DTV_i}{2LV_0}\,(-D) \quad \dots\dots\dots\dots (18)$$

Let's now introduce two more notations, the normalized voltage, defined by $|V_0| = \frac{V_0}{V_i}$. It corresponds to the gain in voltage of the converter, the normalized current, defined by $|I_0| = \frac{L}{TV_i} I_0$. The term $\frac{TV_i}{L}$ is equal to the maximum increase of the inductor current during a cycle; i.e., the increase of the inductor current with a duty cycle D=1. So, in steady state operation of the converter, this means that $|I_0|$ equals 0 for no output current, and 1 for the maximum current the converter can deliver.

Using these notations, we have

in continuous mode $|V_0| = \frac{D}{D-1}$;

in discontinuous mode, $|V_0| = \frac{D^2}{2|I_0|}$;

The current at the limit between continuous and discontinuous mode is $I_{0lim} = \frac{V_i DT}{2L}(1-D)$. Therefore the locus of the limit between continuous and discontinuous modes is given by $\frac{1}{2|I_0|} D(1-D) = 1$.

3. TWO-STAGE PV INVERTER SYSTEM WITH BOOST-TYPE MPPTs

Nowadays, a conventional two-stage configuration is usually adopted in the PV inverter systems. Each MPPT is realized with a boost converter to step up the PV-array voltage close to the specified DC-link voltage, as shown in Figure 2. The boost converter is operated in by-pass mode when the PV-array voltage is higher than the DC-link voltage, However, since the characteristics of PV arrays are different from each other, the inverter operated in by-pass mode cannot track each individual maximum power point accurately, and the inverter suffers from as high-voltage stress as the open voltage of the arrays. To release this limitation, an MPPT topology, which combines buck and boost converters is proposed in this study, in which the control algorithm for tracking maximum power points is based on a perturbation and observation method. The MPPT will switch operation modes between buck and boost when the output voltage of a PV array is close to the DC-bus voltage. The designed controller can switch control laws to achieve smooth mode transition and fulfill online configuration check for the MPPTs, which can be either separate or in parallel connection, to draw the maximum power from the PV arrays more effectively. Additionally, a uniform current control scheme is introduced to the controller to equally distribute the PV array output current to the two MPPTs in parallel operation.

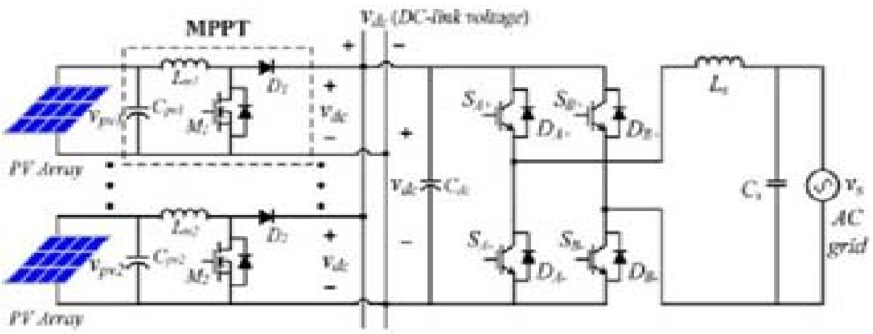

Figure 2. Conventional two-stage PV inverter system with Boost-type MPPTs

To reduce leakage ground current circulating through PV arrays and ground, several transformerless inverter topologies were proposed. Even though they can achieve high efficiency, they require more components than the conventional full-bridge topology. Thus, in this study, the bidirectional full-bridge inverter is operated with bipolar modulation to avoid leakage ground current and to save power components while still sustaining comparatively high efficiency to those in. Note that a full-bridge inverter operated with bipolar modulation can achieve only low frequency common-mode voltage ($V_{CM} = (V_{dc} - V_s)/2$), resulting in low leakage ground current.

To maintain the DC-bus voltage for the grid-connected inverter, the controls, such as robust, adaptive, and fuzzy, were adopted. When adopting these controls for the studied DC-distribution system, a heavy step-load change at the DC-bus side will cause high DC-bus voltage variation and fluctuation, and the system might run abnormally or drop into under or over voltage protection. Bulky DC-bus capacitors can be adopted to increase the hold-up time and suppress the fluctuation of the DC-bus voltage, but it will increase the size and cost of the system significantly. Additionally, even though there are approaches to achieve fast DC-bus voltage dynamics, the systems with load connected to the DC bus have not been studied yet.

4. SIMULATION RESULTS

Open loop system with step change in insolation is shown in Figure 3. Two buck boost converters are connected in parallel to increase the power rating. The step change in input due to increase in the solar energy is shown in Figure 4a. The output voltage of boost converter is shown in Figure 4b. The voltage increases from 320V to 390V. The AC output voltage and load current are shown in Figure 4c and Figure 4d respectively. It can be seen that the steady state error in the output voltage and current is higher.

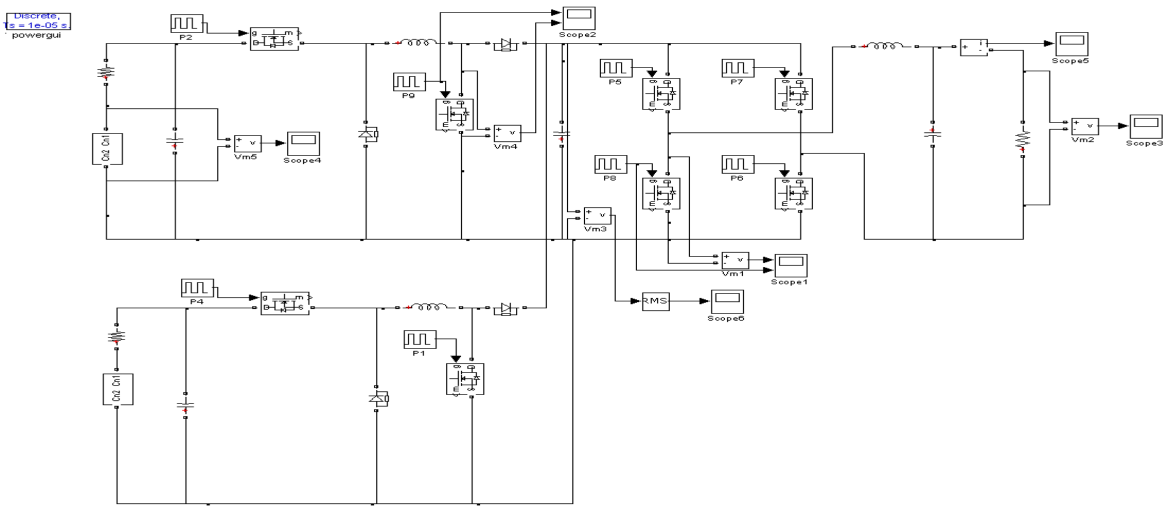

Figure 3. Open loop system

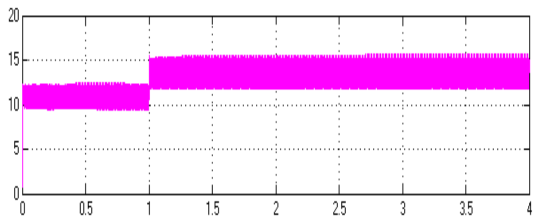

Figure 4a. Input Voltage

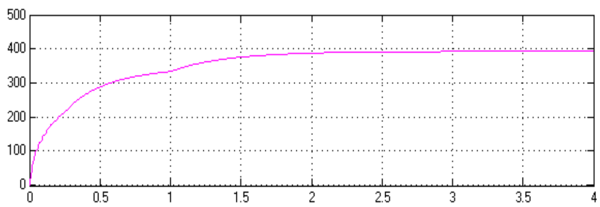

Figure 4b. Output Voltage of Boost Converter

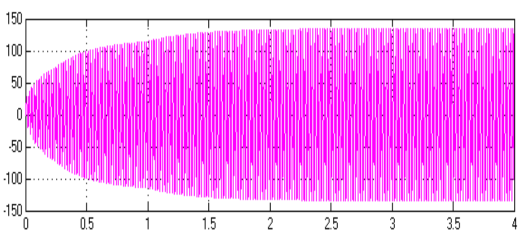

Figure 4c. Output Voltage of Inverter

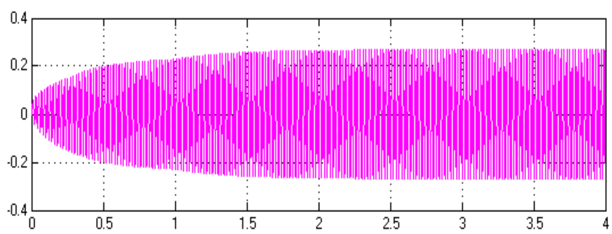

Figure 4d. Output Current of Inverter

Figure 4. Simulation results of the open loop of two buck boost converters

The Simulink diagram of closed loop system is shown in Figure 5. The DC output voltage of the boost converter is sensed and it is compared with the reference voltage. The error is processed using a PI controller. The output of the PI controller is used to update the pulse width applied to the buck boost converter. The step change in input voltage is shown in Figure 6a. The input voltage increases from 10V to 14V. The output of the boost converter is shown in Figure 6b. The output decreases and settles at 240V. The output voltage and current waveforms are shown in Figure 6c and Figure 4d respectively. They are inphase since the load is a resistive load.

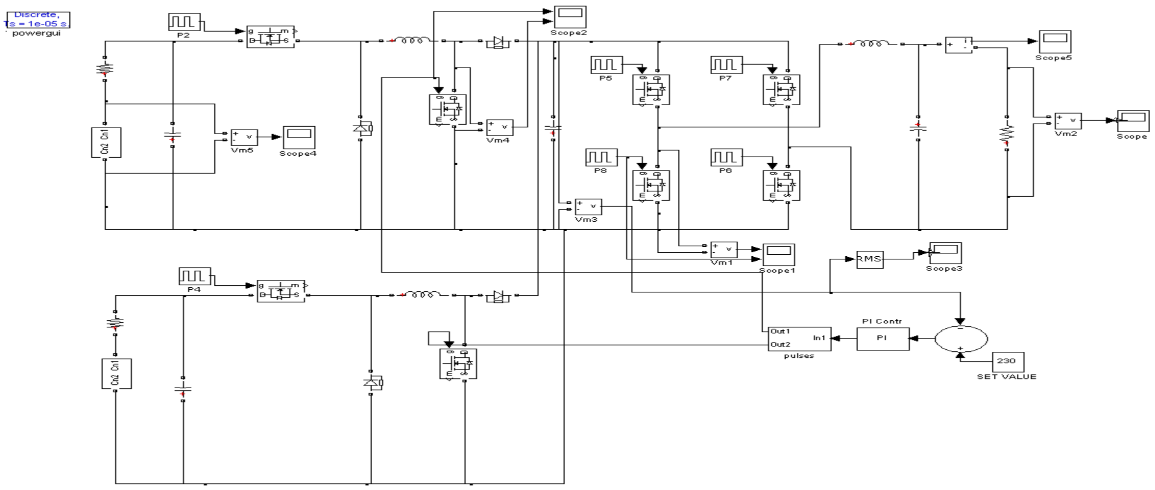

Figure 5. Simulink Model of Closed Loop System

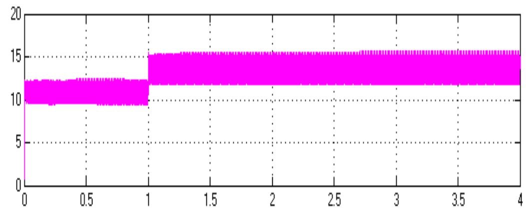

Figure 6a. Input Voltage

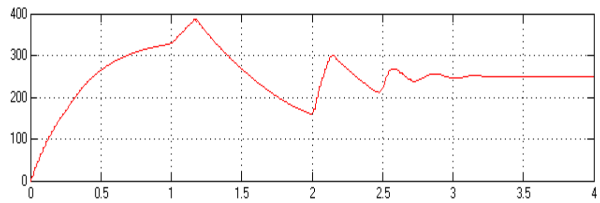

Figure 6b. Output Voltage of the Boost Converter

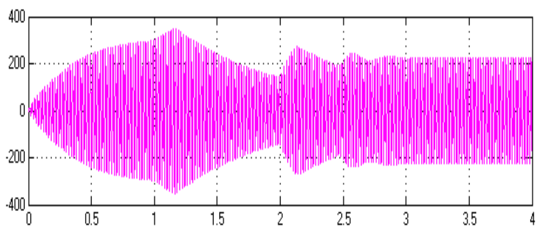

Figure 6c. Output Voltage of the Inverter

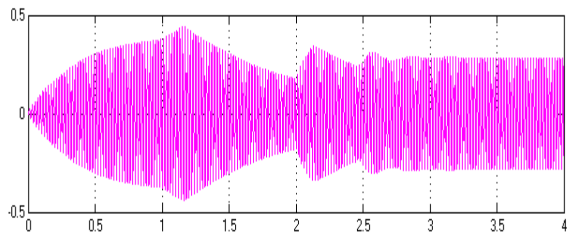

Figure 6d. Output Current of the Inverter

Figure 6. Simulation results of the closed loop of two buck boost converters

5. CONCLUSION

Closed loop controlled parallel cascaded buck boost converter inverter system is successfully modelled and simulated using sim power system. The results of open loop and closed loop systems are presented. The closed loop system is capable of reducing the steady state error. The simulation results are in line with the predications. The closed system has advantages like improved response and reduced steady state error. The disadvantage of this system is that it has limited voltage tracking range. The contribution of this work is to propose a parallel cascaded buck boost converter to improve the npower rating and reduce the inverter input current ripple.

The scope of this work is the simulation of closed loop controlled converter-inverter system with PI controller. The closed loop simulation using fuzzy controller will be done in future.

REFERENCES

[1] L.N. Khanh, J.J. Seo, T.S. Kim and D.J. Won, “Power Management strategies for a grid connected PV-FC hybrid system”, *IEEE Trans. Power Devliv.*, vol. 25, no. 3, pp. 1874-1882, Jul. 2010.
[2] Y.K. Tan and S.K. Panda, “Optimized wind energy harvesting system using resistance emulator and active rectifier for wireless sensor nodes”, *IEEE Trans. Power Electron*, vol. 26, no. 1, pp. 38-50, Jan. 2011.
[3] A. Nami, F. Zare, A. Ghosh, and F. Blaabjerg, “A hybrid cascade converter topology with series-connected symmetrical and asymmetrical diode-clamped H-Bridge cells”, *IEEE Trans. Power Electron*, vol. 26, no. 1, 51–65, Jan. 2011.
[4] S. Dwari and L. Parsa, “An efficient high-step-up interleaved dc–dc converter with a common active clamp”, *IEEE Trans. Power Electron*, vol. 26, no. 1, pp. 66–78, Jan. 2011.
[5] J.M. Shen, H.L. Jou, and J.C. Wu, “Novel transformerless grid connected power converter with negative grounding for photovoltaic generation system”, *IEEE Trans. Power Electron*, vol. 27, no. 4, pp. 1818–1829, Apr. 2012.
[6] T. Kerekes, R. Teodorescu, P. Rodriguez, G. Vazquez, and E. Aldabas, “A new high-efficiency single-phase transformerless PV inverter topology”, *IEEE Trans. Ind. Electron*, vol. 58, no. 1, pp. 184–191, Jan. 2011.
[7] S.V. Araujo, P. Zacharias, and R. Mallwitz, “Highly efficient single-phase transformerless inverters for grid-connected photovoltaic systems”, *IEEE Trans. Ind.Electron*, vol. 57, no. 9, pp. 3118–3128, Sep. 2010.
[8] M.A. Azzouz and A.L. Elshafei, “An adaptive fuzzy regulation of the dc-bus voltage in wind energy conversion systems”, in *Proc. 2010 IEEE Int. Conf. CCA*, pp. 1193–1198.
[9] H. Kakigano, A. Nishino, Y. Miura, and T. Ise, “Distribution voltage control for dc microgrid by converters of energy storages considering the stored energy”, in *Proc. 2010 IEEE ECCE*, pp. 2851–2856.
[10] T.F. Wu, K.H. Sun, C.L. Kuo, and C.H. Chang, “Predictive current controlled 5 kW single-phase bi-directional inverter with wide inductance variation for DC-microgrid applications”, *IEEE Trans. Power Electron*, vol. 25, no. 12, pp. 3076–3084, Dec. 2010.
[11] F. Adamo, F. Attivissimo, A. Di Nisio, and M. Spadavecchia, “Characterization and testing of a tool for photovoltaic panel modeling”, *IEEE Trans.Instrum. Meas*., vol. 60, no. 5, pp. 1613–1622, May 2011.
[12] T.C. Yu and T.S. Chien, “Analysis and simulation of characteristics and maximum power point tracking for photovoltaic systems”, in Proceedings of the International Conference on Power Electronics and Drive Systems (PEDS ’09), pp. 1339–1344, January 2009.
[13] T. Esram and P.L. Chapman, “Comparison of photovoltaic array maximum power point tracking techniques”, *IEEE Trans. Energy Convers*, vol. 22, no. 2, pp. 439–449, Jun. 2007.
[14] Brambilla. A, Gambarara. M, Garutti. A, Ronchi. F, “New Approach to Photovoltaic Arrays Maximum Power Point Tracking”, 30th *Annual IEEE Power Electronics Specialists Conference*, Vol. 2, pp. 632 - 637, 1999.
[15] Honglin Zhou, Shuai Xiao, Geng Yang, Hua Geng, "Modeling and Control for a Bidirectional Buck– Boost Cascade Inverter", *IEEE Transactions on power electronics*, Vol. 27, No. 3, March 2012, pp 1401-1413.
[16] C. Cecati, F. Ciancetta, and P. Siano, "A Multilevel Inverter for Photovoltaic Systems With Fuzzy Logic Control", *IEEE Transactions on Industrial Electronics*, Vol. 57, No. 12, December 2010 pp. 4115-4125.
[17] X.P. Ding, Z.M. Qian, S.T. Yang, B. Cui, and F.Z. Peng. “A Direct DC-link Boost Voltage PID-like Fuzzy Control Strategy in Z-Source Inverter”, *IEEE*, 2008, pp. 405-411.
[18] Y.H. Chang and C.Y. Chang, "A Maximum Power Point Tracking of PV System by Scaling Fuzzy Control", presented at *International Multi Conference of Engineers and Computer Scientists*, Hong Kong, 2010.
[19] Oscar Lopez-Lapena, Maria Teresa Penella, and Manel Gasulla. 2012. “A closed -Loop Maximum power point Tracker for Sub watt Photovoltaic Panels”. *IEEE Transactions on Industrial Electronics*. 59(3).
[20] Shuai Jiang, Dong Cao, Yuan Li and Fang Zheng Peng. 2012. “Grid - Connected Boost-Half-Bridge Photovoltaic Micro inverter System Using Repetitive Current Control and Maximum power point tracking”. *IEEE Transactions on power Electronics*. 27(11).
[21] Abdullah Abusorrah, Mohammed. M., Al-Hindawi, Yusuf Al-Turki, Kuntal Mandal, Damian Giaouris, Soumitro Banerjee, Spyros Voutetakis and Simira Papadopoulou. 2013. “Stability of a boost converter fed from a photovoltaic source”. *Solar energy*. 98: 458-471.
[22] Sairaj V. Dhople, Ali Davoudi, Alejandro D. Dominguez-Garcia and Patrick L. Chapman. 2012. “A unified Approach to Reliability Assessment of Multiphase DC-DC Converters in Photovoltaic Energy Conversion Systems”. *IEEE Transactions on power Electronics*. 27(2).
[23] Shih-Ming Chen, Tsorng Juu, Liang, Lung Sheng and Jiann Fuh Chen. 2012. “A safety enhanced high stepup DC-DC Converter for AC Photovoltaic Module Application”. *IEEE Transactions on power electronics*. 27(4).
[24] Stephane vighetti, jean-Paul ferrieux and Y veslembeye. 2012. “Optimization and design of a cascaded DC/DC Converter Devoted to gridconnected photovoltaic System”. *IEEE Transaction on power electronics*. 27(4).
[25] Chong B.V. P and Zhang. L. 2012. “Controller design for integrated PV-converter modules under partial shading conditions”. *Solar energy*. 92: 123-138.

BIOGRAPHIES OF AUTHORS

T. Sundar is a Research Scholar in the Dept. of EIE, SCSVMV University, Kanchipuram. He is doing research in the field of PV system using Advanced Instrumentation System. He is a research scholar in SCSVMV University. His area of interest is PV Systems and their Control.

S. Sankar obtained his B.E Degree in Electrical & Electronics Engineering at Sri Venkateswara College of Engineering, from Madras University and M.E (Power System) Degree from Annamalai University Chidambaram. He has done his Ph.D in the area of FACTS controllers. His research interests are in the area of FACTS and PV systems. He has published papers on IPFC and Converter.